Turkish J. Eng. Env. Sci.
36 (2012) , 179 – 194.

doi:10.3906/muh-1104-9

# In-situ stress measurements by hydraulic fracturing method at Gotvand Dam site, Iran

**Reza ZIAIE MOAYED**[1,*], **Ehsan IZADI**[2], **Mohsen FAZLAVI**[3]
[1] *Civil Engineering Department, Imam Khomeini International University, Qazvin-IRAN*
*e-mail: R_ziaie@ikiu.ac.ir*
[2] *Civil Engineering Department, Imam Khomeini International University, Qazvin-IRAN*
[3] *Earthquake Research Center, Tehran - IRAN*

Received: 13.04.2011

**Abstract**

A set of hydraulic fracturing tests were conducted for determining in situ stresses in 10 inclined and vertical boreholes ranging in depth from 30 to 100 m at locations of hydropower plant tunnels of the Gotvand Dam site in the southwest of Iran. The rock in the studied area is formed by the sequence of sandstone, clay stone, and mudstone layers of the Aghajari (AJ) formation, and by thick conglomerate layers of the Bakhtiari (BK) formation. Note that the AJ formation is located underneath the BK formation. The in situ tests were carried out by using conventional systems with special high pressure rods and straddle packer tools. The tests were conducted both in fractured and intact rocks. The measurements yielded an orientation of the maximum horizontal stress of N $30^\circ \pm 5^\circ$ (NE-SW), which is generally the same as directions indicated by focal mechanisms solutions from earthquakes and fault conditions in the location of the area studied.

**Key Words:** Gotvand Dam, in situ stress, hydraulic fracturing test

## 1. Introduction

Knowledge of field stresses is very important in many problems dealing with rocks in civil, mining, and petroleum engineering. The modern rock mechanics engineer has to be well acquainted with the basis of rock stresses and rock stress measurements. The need for understanding in situ stresses in rocks has been recognized by geologists and engineers for a long time and many methods have been proposed to measure these stresses since the early 20th century.

Hydraulic injection stress measurements for determining in situ underground stresses are used in different areas such as dam and tunnel construction, earthquake prediction, and oil and gas source designing all over the world (Haimson and Fairhurst, 1970; Cornet and Julien, 1989; Ziaie Moayed et al., 2008; Jeffrey et al., 2010).

The appeal of hydraulic fracturing test (HFT) for in situ stress measurements comes from its relatively simple operation and easy interpretation. This technique was first introduced by Clark in 1949. Then it was developed by Hubbert and Willis (1957), Scheidegger (1962), Kehle (1964), Fairhurst (1964), Haimson

*Corresponding author

and Fairhurst (1967 and 1970), Fairhurst (1974), and some others. This technique consists of creating a hydraulic fracture inside a borehole by injecting a fluid inside the sealed interval and determining the mechanical characteristics of rock such as shut-in pressure of fractures and tensile strength of rock.

Different methods of fracturing such as hydraulic test on intact or preexisting fractures, sleeve fracturing, and hydro jacking are designed to study the behavior of principal stresses by means of hydraulic concepts (Baumgärtner and Rummel, 1989).

Several studies have been carried out on hydraulic fracturing methods in Iran. Ajalloeian et al. (2011) reported the results and evaluation of hydraulic jacking and hydraulic fracturing tests conducted on the Aghajari (AJ) formation in different depths. Shadizadeh et al. (2009) performed hydraulic fracturing tests on a Bangestan reservoir site, Ahwaz. They performed an extreme test program to find the best layer to perform hydraulic fracturing tests. They stated that the Ilam formation could be a good candidate for this.

The aim of this study was to analyze and assess the results of hydraulic fracturing tests at the Gotvand Dam site, Iran, to determine the magnitude and orientation of the principal stresses.

## 2. General geology of the region

The Gotvand Dam site is located on the AJ and Bakhtiari (BK) formations as shown in Figure 1. AJ is mainly formed by the sequence of brownish to grayish sandstones with clay stone inter-bedded layers and siltstones. The BK formation is generally formed by thick conglomerate layers with lime and silica cement. These thick layers are generally separated by sandstone and claystone interbedded layers. The rock in the area studied is mainly formed by the sequence of AJ layers, especially the mudstone and siltstone layers. Furthermore, the fault is perpendicular to the dam axes (Ziaie Moayed et al., 2008).

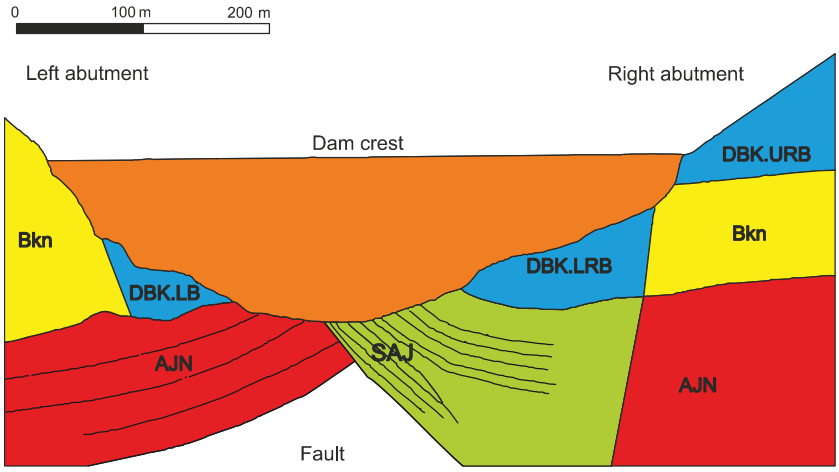


**Figure 1.** Geological profile in dam axis.

## 3. Drilling and sampling

Borehole drillings and hydraulic fracturing tests were carried out at 3 separate stations of the hydropower plant tunnels of the Gotvand Dam site. The locations of these stations (marked T2, YB, and LP) are shown in Figure 2.

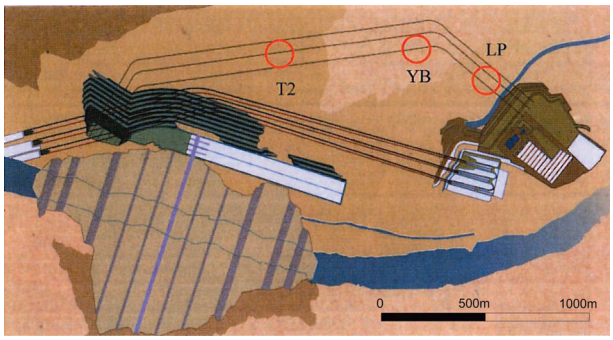


**Figure 2.** Locations of hydropower plant tunnels of the Gotvand Dam site and test stations of HFT.

Ten boreholes ranging in depth from 30 to 100 m were drilled to explore the features of underground layers and to conduct hydraulic fracturing tests. More information related to the boreholes is given in Table 1. A drilling machine (SD300) capable of drilling vertical and horizontal boreholes was used (Figure 3). The applied drilling method was continuous coring with a diameter of 101 mm.

**Figure 1.** Depth and orientation of the boreholes in Gotvand Dam for HFT.

| No. | Station | Borehole | DIP | Plunge Direction | Borehole length (m) |
|---|---|---|---|---|---|
| 1 | LP | LPHF1 | 90 | — | 60 |
| 2 | | LPHF2 | 0 | — | 60 |
| 3 | | LPHF3 | 90 | — | 55 |
| 4 | YB | YBHF1 | 90 | — | 50 |
| 5 | | T2HF | 90 | — | 100 |

**Figure 3.** Drilling machine (SD300) while drilling horizontal borehole.

The YB and T2 stations' elevation is equal to the tunnel level and the LP station has a lower elevation than river level. This difference between tunnel level and river level is about 80 m as illustrated in Figure 4.

As shown in Figure 4, the overburden of each station is equal to 70 m, 130 m, and 240 m for LP, YB, and T2 stations, respectively. It may be expected that the principal stress orientations are affected by the magnitudes of different overburden stresses at the stations.

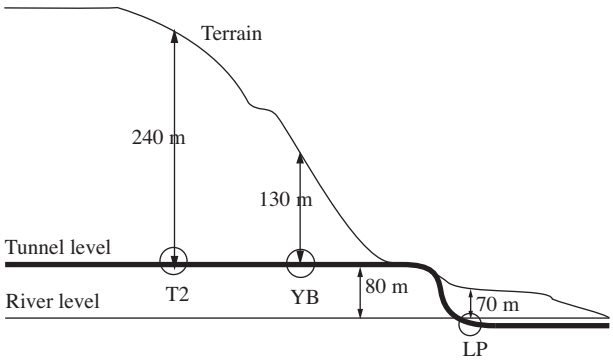


**Figure 4.** Comparison between tunnel and river level at the LP, YB, and T2 stations.

## 4. Test equipment and methodology

The hydraulic fracturing test (HFT) and hydraulic test in pre-existing fracture (HTPF) at the Gotvand site were carried out using the main engineering equipment including:

- Three-piston electromotor pumps with controlled pressure capacity and flow of maximum 350 Pa and 1 $m^3/s$, respectively.
- Hydraulic fracturing double packer with 95 mm diameter with the capacity of maximum pressure of 450 Pa.
- Ultrasonic flow meter
- Pressure sensor and data logger
- High pressure hoses and sealing rods capable of tolerating high water pressure
- Impression packer and pertinent items used to observe fractures and their orientation
- Borehole camera and compass
- Other accessories and tools such as container, winch, air compressor.

Some of the pieces of equipment used are shown in Figure 5.

The test procedure followed exactly the ASTM standard and ISRM suggested method (ASTM D4645, 1992; Haimson et al., 2003; Haimson and Cornet, 2003; Hanson, 2004).

Suitable test sections in each borehole were selected on the basis of the analysis of the rock core material and borehole logs. For HFT, homogeneous borehole sections without visible fractures were selected and, for HTPF tests, fractured sections mainly with different spatial orientation were selected.

After the installation of the equipment and the packer to the desired depth, the tests started with the following steps (Klee and Rummel, 2004):

- The packer inflated to a pressure of 49-59 Pa.

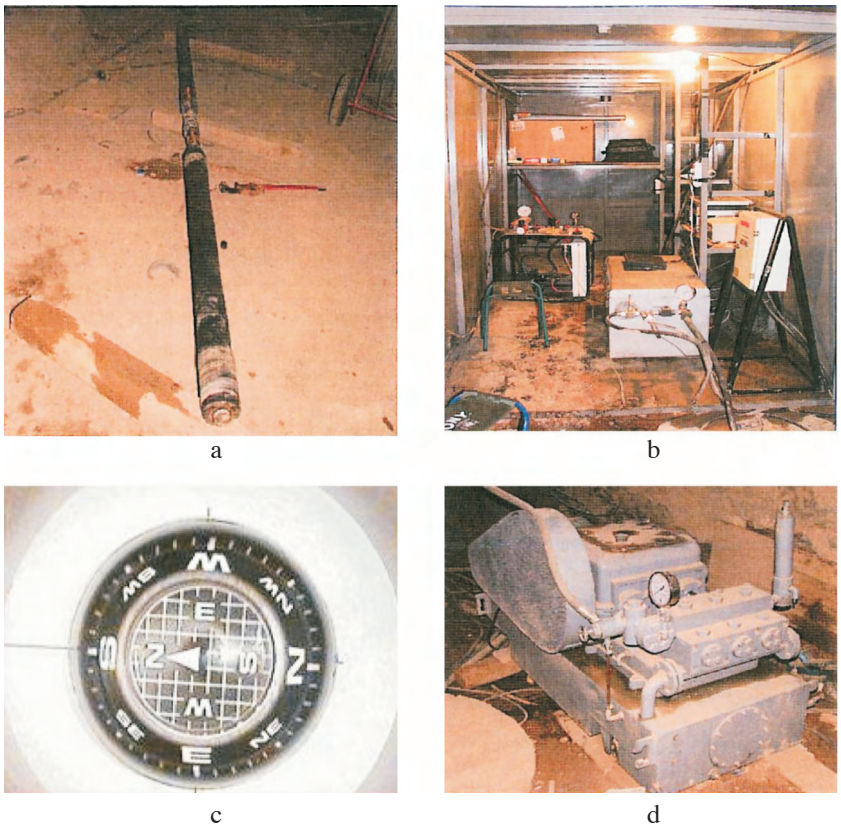


**Figure 5.** Some of the hydraulic fracturing test equipment. (a): Double packers; (b): Control room; (c) Borehole compass; (d): Main pump.

- The test interval pressurized rapidly to a pressure of about 20 Pa, and subsequently decayed for about 5 min in the case of HFT, and for about 15 min in the case of HTPF. Then interval pressure released. This is a permeability test, which is marked as first "P-test" in this study.
- The test interval pressurized with an injection rate ranging from 0.06 to 0.12 $m^3/s$. The pressure inside of the test interval increases. This happens because the volume of the test interval before initiation of any fracture remains constant. In the case of HFT, increasing pressure continues until a fracture occurs inside the borehole, while in the case of HTPF this procedure continues up to a time of about 1 min.
- Injection and system shut-in terminated after about 3 min.
- The interval pressure released and the recovered fluid volume observed.
- In order to observe the shut-in pressure of fractures, several repetitions of re-pressurization of the test interval with constant injection rate of about 0.12-0.3 $m^3/s$ for about 1 min done.
- Injection and system shut-in terminated after about 3 min.
- The interval pressure released and the recovered fluid volume observed.

- A step-rate injection test with stepwise increase in the injection flow-rate conducted and the corresponding injection pressure observed.
- Injection and system shut-in terminated after about 3 min.
- The interval pressure released and the recovered fluid volume observed.
- The final step-rate test conducted as usually done for the classical Lugeon test, referred to in this study as "SP-test" (second permeability test).
- Finally, the packer deflated and prepared for the next test section.

## 5. Test results and discussion

### 5.1. Analysis and interpretation of HFT results

During each test, the injection pressure and injection flow rate and the recovered fluid volume were recorded by the digital data acquisition system. The derived parameters of HFT (breakdown pressure at the moment of fracture initiation, $P_c$; fracture re-opening pressure, $P_r$; shut-in pressure, $P_{si}$; and the resulting in situ tensile strength, $P_{co}$) as well as the results of the impression packer tests (fracture strike direction, $\theta$; dip direction, $\beta$; and dip, $\alpha$) in the boreholes are summarized in Table 2. It is important to note that during the tests for the borehole no. LPHF2 the packer failed and the continuation of the test was interrupted; thus the complete data for LPHF2 are not available.

For instance, the analysis of the graphical test record at a depth of 36 m at the YB station, borehole no. YBHF1 is shown in Figure 6. In this diagram, the pressure-time plot and methods for determination of $P_c$, $P_r$, and $P_{co}$ are shown.

The shut-in pressure $P_{si}$ was determined by the following 3 steps (Guo et al., 1993):

- The plot of pressure-injection flow-rate allows one to determine the exact pressure value at which the hydraulic flow terminates (Q = 0). Therefore, the P-Q plot yields an upper-limit estimate of the shut-in pressure ($P_{si(\max)}$ in Table 2).
- A Muskat-type plot of the logarithm of the difference between the pressure P and an asymptotic pressure level $P_a$ vs. time t yields the lower-limit of the shut-in pressure ($P_{si(\min)}$ in Table 2.) , assuming that the linear part of the plot characterizes radial flow, i.e. the stimulated fracture is nearly closed.
- These 2 limits of shut-in pressure, which indicate acting stress normal to the fracture plane, mark a transition from a rapid linear pressure drop, observed immediately after shut-in, to the beginning of a diffusion-dominated slow pressure decrease. This transition can be determined by a tangent to the linear pressure decrease known inflection point in the pressure-time plot ($P_{si(\text{average})}$ in Table 2.). This approach was proposed by Gronseth and Kry (1981).

The derived characteristic pressure data ($P_c$, $P_r$, $P_{si}$, $P_{co}$) against true vertical depth (TVD), are shown graphically in Figure 7 to Figure 10, respectively. Note that the fracture initiation pressures of all the boreholes increased with increase in depth.

**Table 2.** Results of hydraulic injection tests in Gotvand Dam, $P_c$: fracture initiation pressure, $P_r$: fracture re-opening pressure, $P_{co}$: in situ hydraulic tensile strength, $P_{si}$: shut-in pressure, $\theta$: strike of fracture plane (north over east), $\beta$: dip direction of fracture plane (north over east), $\alpha$: dip of fracture plane (with respect to horizontal).

| Station | Borehole | Material | Borehole length (m) | Pc (MPa) | | Pr (MPa) | Pco (MPa) | Psi (MPa) | | | Orientation | | |
|---|---|---|---|---|---|---|---|---|---|---|---|---|---|
| | | | | HF | HFPF | | | Average | Min | Max | θ | β | α |
| LP | LPHF1 | Silt stone | 26.5 | | 7.97 | 3.18 | 4.74 | 2.50 | | | 30 | 120 | 75 |
| | | Silt stone | 35.5 | | 7.50 | 3.00 | 4.40 | 2.20 | | | | | |
| | | Silt stone | 43.5 | | 7.33 | 2.92 | 3.93 | 3.00 | | | | | |
| | | Sand stone | 46.0 | | 8.78 | 3.70 | 4.28 | 2.43 | | | | | |
| | | Silt stone | 52.3 | | 8.73 | 3.50 | 5.13 | 2.52 | | | | | |
| | LPHF2 | Silt stone | 43.0 | | 10.38 | Failed | Failed | Failed | Failed | Failed | | | |
| | LPHF3 | Clay stone | 22.5 | | 6.70 | 2.23 | 4.27 | 1.80 | | | 20 | 110 | 63 |
| | | Clay stone | 24.5 | | 6.94 | 3.00 | 3.69 | 2.27 | | | 30 | 120 | 20 |
| | LPHF4 | Clay stone | 21.5 | | 5.40 | 1.90 | 3.40 | 1.38 | | | 340 | 70 | 70 |
| | | Silt stone | 24.0 | | 6.95 | 3.70 | 3.02 | 2.36 | | | | | |
| | LPHF5 | Clay stone | 46.1 | | 8.73 | 2.46 | 6.03 | 2.43 | | | | | |
| | LPHF6 | Silt stone | 33.5 | | 8.10 | 4.10 | 3.98 | 2.73 | | | 10 | 100 | 0 |
| | | Silt stone | 40.7 | 16.75 | | 3.00 | 13.25 | 2.04 | | | 40 | 130 | 55 |
| YB | YBHF1 | Silt stone | 31.0 | 14.77 | | 2.03 | 12.47 | 1.93 | 1.79 | 1.96 | 30 | 120 | 83 |
| | | Silt stone | 36.0 | 15.26 | | 2.04 | 12.36 | 2.08 | 1.98 | 2.08 | 10 | 100 | 85 |
| | | Sand stone | 38.8 | | 6.12 | 2.14 | 3.72 | 2.35 | 2.14 | 2.36 | 48 | 318 | 20 |
| | | Clay stone | 42.5 | 14.61 | | 2.10 | 12.11 | 1.89 | 1.83 | 1.90 | 172 | 82 | 80 |
| | | Silt stone | 47.3 | | 7.08 | 2.25 | 4.63 | 2.23 | 2.08 | 2.23 | 5 | 275 | 15 |
| | YBHF2 | Sand stone | 22.0 | | 5.38 | 1.41 | 3.82 | 1.50 | 1.30 | 1.51 | 1 | 91 | 37 |
| | | Clay stone | 24.5 | | 6.53 | 1.83 | 4.43 | 1.53 | 1.24 | 1.61 | 28 | 118 | 82 |
| | | Silt stone | 28.5 | | | 1.33 | | 1.29 | 1.03 | 1.29 | 172 | 82 | 32 |
| | | Silt stone | 30.9 | | 6.09 | 1.27 | 4.49 | 1.35 | 1.19 | 1.34 | 5 | 95 | 33 |
| | | Silt stone | 34.0 | | 5.68 | 1.74 | 4.08 | 1.65 | 1.56 | 1.70 | 88 | 358 | 47 |
| | YBHF3 | Silt stone | 25.4 | | 2.92 | 1.25 | 1.43 | 1.17 | 1.09 | 1.22 | 15 | 285 | 66 |
| | | Silt stone | 29.0 | | 7.88 | 1.64 | 6.28 | 1.64 | 1.59 | 1.70 | 7 | 97 | 68 |
| | | Silt stone | 32.8 | | | 1.75 | | 1.75 | 1.65 | 1.75 | 88 | 358 | 65 |
| | | Silt stone | 35.5 | 13.22 | | 2.10 | 11.47 | 2.00 | 1.93 | 2.01 | 177 | 266 | 48 |
| T2 | T2HF1 | Silt stone | 23.4 | | 7.9 | 4.4 | 3.9 | 2.8 | 2.3 | 2.4 | | | |
| | | Conglomerate | 28.5 | | 6.0 | 4.5 | 1.5 | 2.0 | 1.2 | 2.6 | | | |
| | | Conglomerate | 37.5 | | 5.5 | 4.2 | 1.3 | 2.3 | 1.0 | 2.8 | | | |
| | | Conglomerate | 39.5 | | 5.9 | 4.3 | 1.6 | 2.4 | 1.1 | 2.5 | | | |
| | | Conglomerate | 42.5 | | 5.6 | 4.6 | 1.1 | 3.0 | 1.2 | 3.0 | | | |
| | | Sand stone | 83.5 | 17.1 | | 7.1 | 10 | 4.3 | 2.9 | 4.8 | 30 | 120 | 90 |
| | | Sand stone | 85.5 | 14.3 | | 5.4 | 8.9 | 3.8 | 3.0 | 3.9 | 60 | 150 | 85 |
| | | Sand stone | 91.6 | 11.3 | | 4.5 | 6.8 | 3.8 | 3.8 | 4.1 | | | |

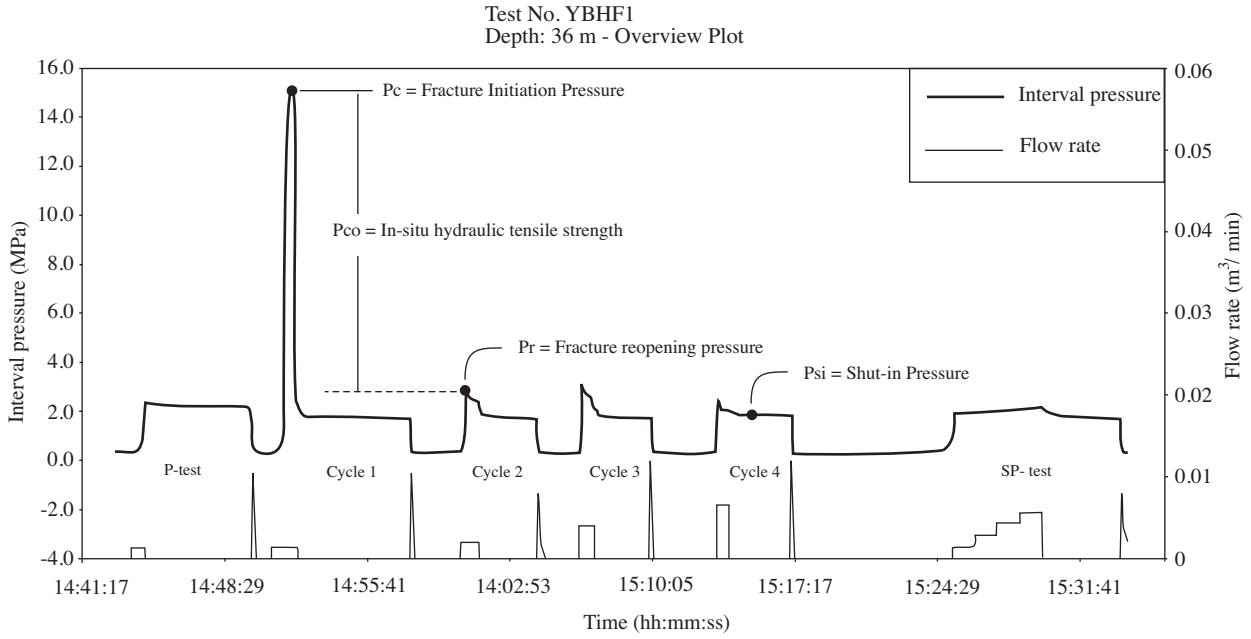


**Figure 6.** Graphical diagram of HFT result at the YB station at Gotvand Dam site (borehole no. YBHF1-depth: 36 m).

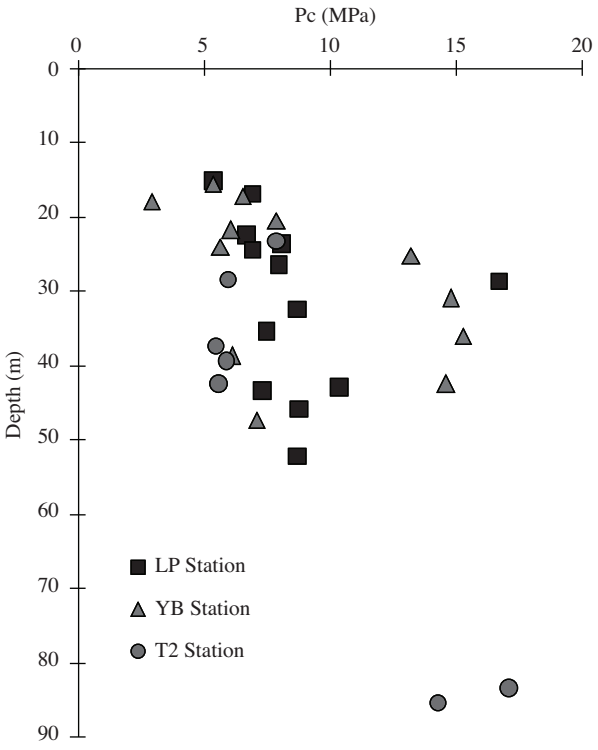


**Figure 7.** Breakdown pressure Pc at Gotvand Dam site.

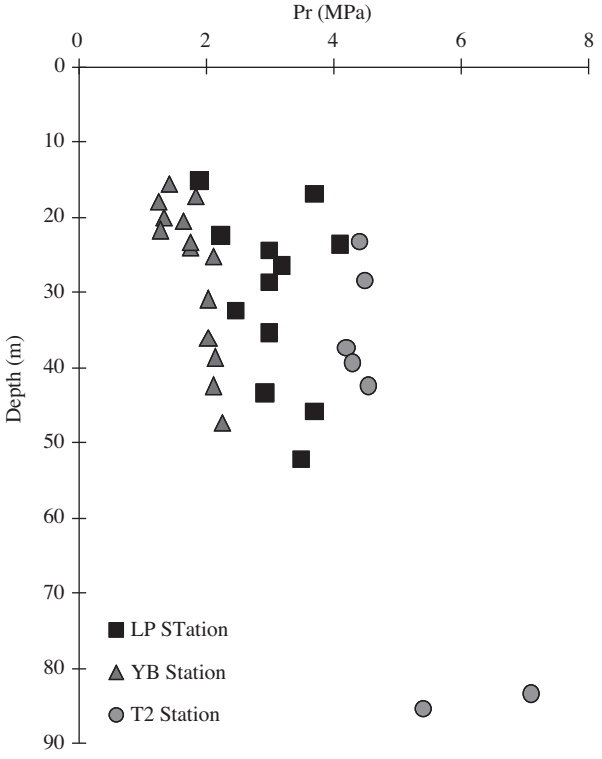


**Figure 8.** Fracture re-opening pressure (Pr) at Gotvand Dam site.

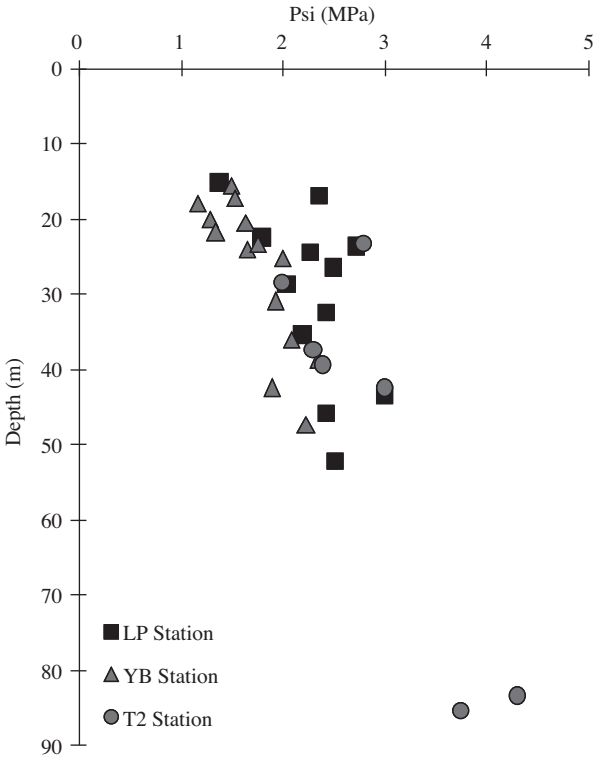


**Figure 9.** Shut-in pressure (Psi) at Gotvand Dam site.

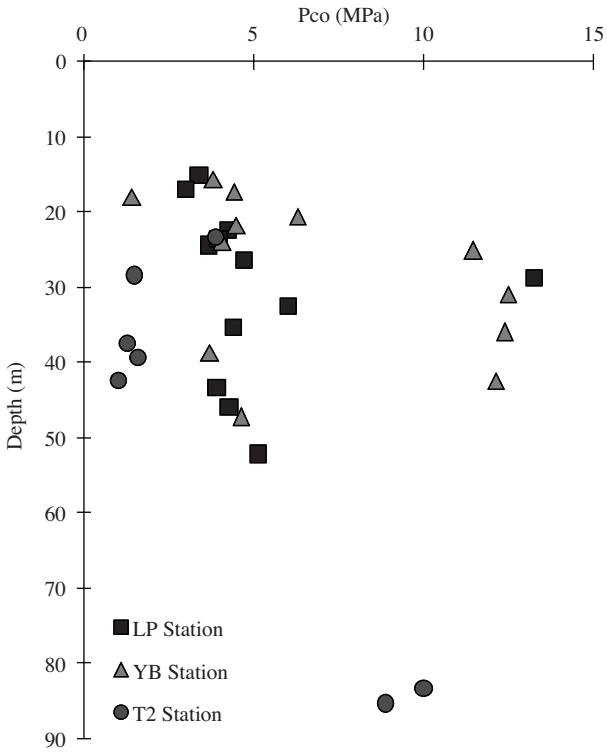


**Figure 10.** In situ tensile strength (Pco) at Gotvand Dam site.

### 5.2. Tracing of the fracture

After completion of all HFT and HTPF, the straddle packer tool was replaced by the impression packer. The impression packer tests consisted of an inflation of the impression packer element to a pressure approximately 20% above the fracture re-opening pressure for a time of about 30 min. After recovery of the packer tool to the surface, the fracture trace is marked on the packer sleeve and reflected to a transparent plastic cover sheet wrapped around the packer. The captured pictures from the borehole camera and compass unit provide the orientation of the reference mark with respect to magnetic north. Examples of the fracture traces observed during impression packer testing are shown in Figure 11.

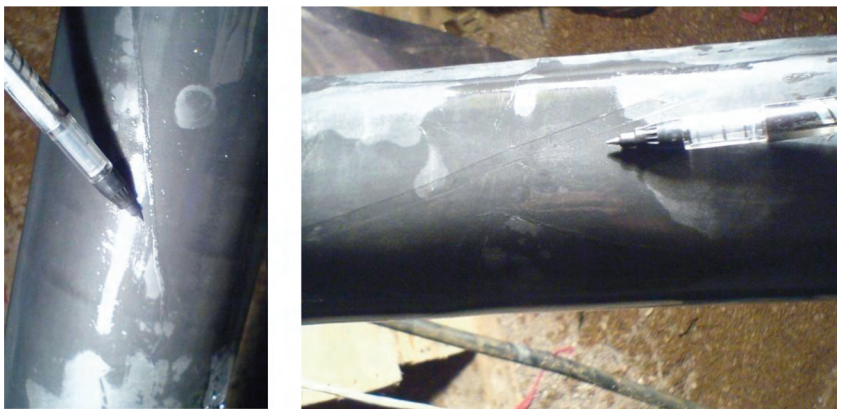

**Figure 11.** Effect of HF crack on impression packer plastic cover at YB station of Gotvand.

Using the above method, all the hydraulic fracturing tests and hydraulic injection tests in pre-existing fractures as well as impression packer tests for fracture orientation determination were carried out in the AJ and BK formation boreholes.

### 5.3. Stress evaluation from hydraulic fracturing tests

To derive stresses from measurements in boreholes, it is necessary to consider the stress distribution around a circular hole subjected to far-field compressive stresses. This solution was first derived by Kirsch (1898). In the case where the borehole axis is parallel to the maximum principal stress, the Hubbert and Willis formula for the critical pressure $\mathrm{P}_c$ at the moment of fracture initiation is used (Hubbert and Willis, 1957; Haimson and Fairhurst, 1970):

$$P_c = 3.S_h - S_H + P_{co} - P_p \tag{1}$$

where $\mathrm{S}_h$ and $\mathrm{S}_H$ are the horizontal far-field principal stresses, $\mathrm{P}_{co}$ is the in situ tensile strength of the rock, and $\mathrm{P}_p$ is the pore pressure in the rock mass. $\mathrm{P}_c$ is often called the breakdown pressure during the hydraulic fracturing process. It is assumed that the vertical stress is a principal stress and equal to the overburden stress, and the rock is homogeneous, isotropic, and initially impermeable, and that the induced fracture is oriented perpendicular to the minimum horizontal principal stress $\mathrm{S}_h$. The last assumption yields:

$$P_{si} = S_h \tag{2}$$

where $\mathrm{P}_{si}$ is the shut-in pressure to merely keep the fracture open after the pressurizing system. After pressure release, the fracture may close. It can be re-opened during subsequent pressure cycles at a pressure of:

$$P_r = 3.S_h - S_H - P_p = P_c - P_{co} \tag{3}$$

Using this linear elastic approach, the principal stresses can be expressed by the relations:

$$\begin{aligned} S_h &= P_{si} \\ S_H &= 3.P_{si} - P_r - P_p \\ S_v &= \rho.g.z \\ P_{co} &= P_c - P_r \end{aligned} \tag{4}$$

Thus, the stress analysis only requires knowledge of the rock mass density, $\rho$, the determination of characteristic pressure values in particular the shut-in pressure, $\mathrm{P}_{si}$, and re-opening pressure, $\mathrm{P}_r$, at depth z where the fracture is produced.

Considering the simple and idealistic assumptions used in the above approach, the determination of stresses by Eqs. (4) may sometimes be questioned. This, in particular, applies to the assumptions on rock mass isotropy.

The resulting minimum and intermediate principal stresses, $\mathrm{S}_h$ and $\mathrm{S}_H$, are listed in Tables 3 to 5, and are shown graphically in Figures 12 to 14, for stations LP, YB, and T2, respectively. For vertical stress calculation an average value of about 2.480 g/cm$^3$ was considered, according to the results of experiments on the rock density.

**Table 3.** Results of the stress evaluation using the Hubbert and Willis (1957) approach at the LP station, Gotvand Dam.

| Borehole no. | Test code | Borehole length (m) | Sh (MPa) | SH (MPa) | SV (MPa) | $\theta$ for SH (deg) |
|---|---|---|---|---|---|---|
| LPHF1 | LPHF1-26.5 | 26.5 | 2.5 | 4.3 | 2.6 | N30E |
| | LPHF1-35.5 | 35.5 | 2.2 | 3.6 | 2.9 | - |
| | LPHF1-43.5 | 43.5 | 3.0 | 6.1 | 3.1 | - |
| | LPHF1-46 | 46.0 | 2.4 | 3.6 | 3.1 | - |
| | LPHF1-52.25 | 52.3 | 2.5 | 4.1 | 3.3 | - |
| LPHF3 | LPHF3-22.5 | 22.5 | 1.8 | 3.2 | 2.5 | N20E |
| | LPHF3-24.7 | 24.7 | 2.3 | 3.8 | 2.6 | N30E |
| LPHF4 | LPHF4-21.5 | 21.5 | 1.4 | 2.2 | 2.4 | - |
| | LPHF4-24 | 24.0 | 2.4 | 3.4 | 2.4 | - |
| LPHF5 | LPHF5-46.1 | 46.1 | 2.4 | 4.8 | 2.8 | N0E |
| LPHF6 | LPHF6-33.5 | 33.5 | 2.7 | 4.1 | 2.6 | N10E |
| | LPHF6-40.7 | 40.7 | 2.0 | 3.1 | 2.7 | N20E |

**Table 4.** Results of the stress evaluation using the Hubbert and Willis (1957) approach at the YB station, Gotvand Dam.

| Borehole no. | Test code | Borehole length (m) | Sh (MPa) | SH (MPa) | SV (MPa) | $\theta$ for SH (deg) |
|---|---|---|---|---|---|---|
| YBHF1 | YBHF1-d31 | 31 | 1.93 | 3.76 | 3.9928 | N30E |
| | YBHF1-d36 | 36 | 2.08 | 4.2 | 4.1168 | N103 |
| | YBHF1-d38.8 | 38.8 | 2.35 | 4.91 | 4.1862 | N48E |
| | YBHF1-d42.5 | 42.5 | 1.89 | 3.57 | 4.278 | N172E |
| | YBHF1-d47.3 | 47.3 | 2.23 | 4.44 | 4.397 | N5E |
| YBHF2 | YBHF2-d22 | 22 | 1.5 | 3.09 | 3.6109 | N1E |
| | YBHF2-d24.5 | 24.5 | 1.53 | 2.76 | 3.653 | N28E |
| | YBHF2-d28.5 | 28.5 | 1.29 | 2.54 | 3.7225 | N172E |
| | YBHF2-d30.9 | 30.9 | 1.35 | 2.78 | 3.7646 | N5E |
| | YBHF2-d34 | 34 | 1.65 | 3.21 | 3.8192 | - |
| YBHF3 | YBHF3-d25.4 | 25.4 | 1.17 | 2.26 | 3.6704 | N15E |
| | YBHF3-d29 | 29 | 1.64 | 3.28 | 3.7349 | N7E |
| | YBHF3-d32.8 | 32.8 | 1.75 | 3.5 | 3.7994 | - |
| | YBHF3-d35.5 | 35.5 | 2 | 3.9 | 3.849 | N177E |

**Table 5.** Results of the stress evaluation using the Hubbert and Willis (1957) approach at the T2 station, Gotvand Dam.

| Borehole no. | Test code | Borehole length (m) | Sh (MPa) | SH (MPa) | SV (MPa) | $\theta$ for SH (deg) |
|---|---|---|---|---|---|---|
| T2-1 | T2-1-23.4 | 23.4 | 2.8 | 4 | 6.532 | - |
| | T2-1-28.5 | 28.5 | 2 | 1.5 | 6.659 | - |
| | T2-1-37.5 | 37.5 | 2.3 | 2.7 | 6.882 | - |
| | T2-1-39.5 | 39.5 | 2.4 | 2.9 | 6.932 | - |
| | T2-1-42.5 | 42.5 | 3 | 4.45 | 7.006 | - |
| | T2-1-83.3 | 83.3 | 4.3 | 5.8 | 8.018 | N30E |
| | T2-1-85.6 | 85.5 | 3.75 | 5.85 | 8.075 | N60E |
| | T2-1-91.6 | 91.6 | 3.75 | 6.75 | 8.224 | - |

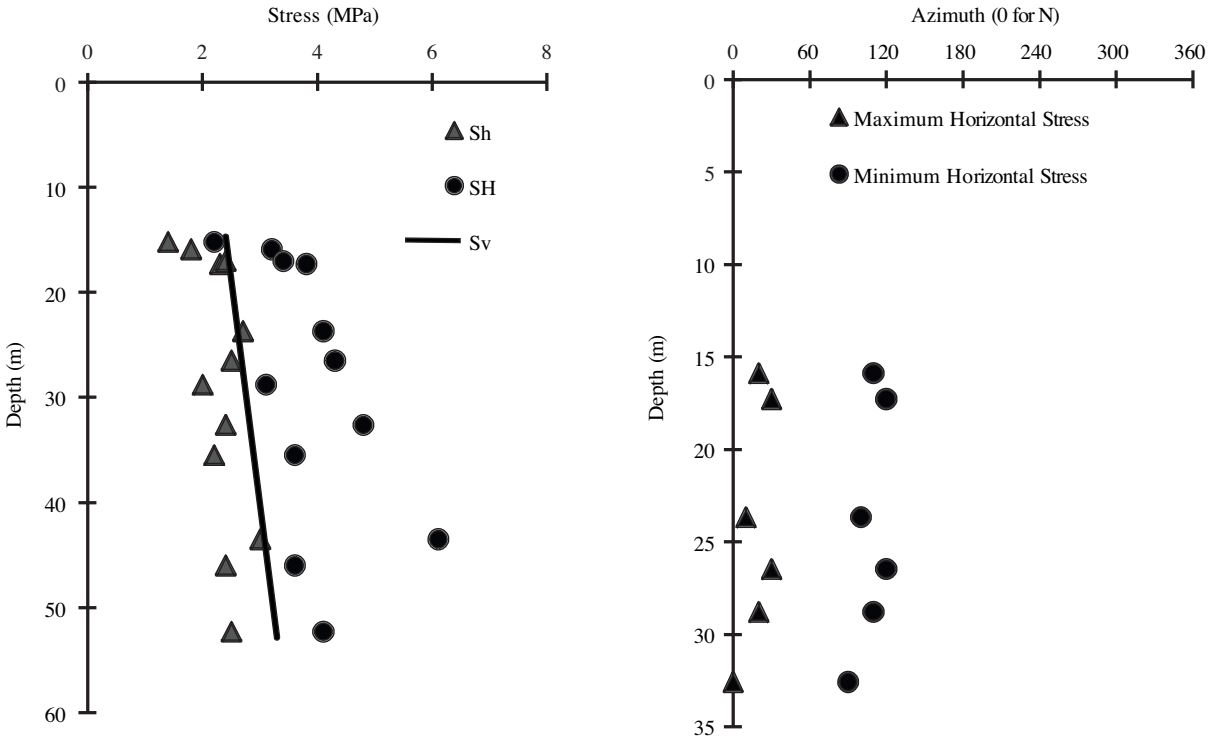


**Figure 12.** Principal stress interpretations at the LP station: (a) Principal stress vs. depth; (b) Horizontal stress orientation vs. depth

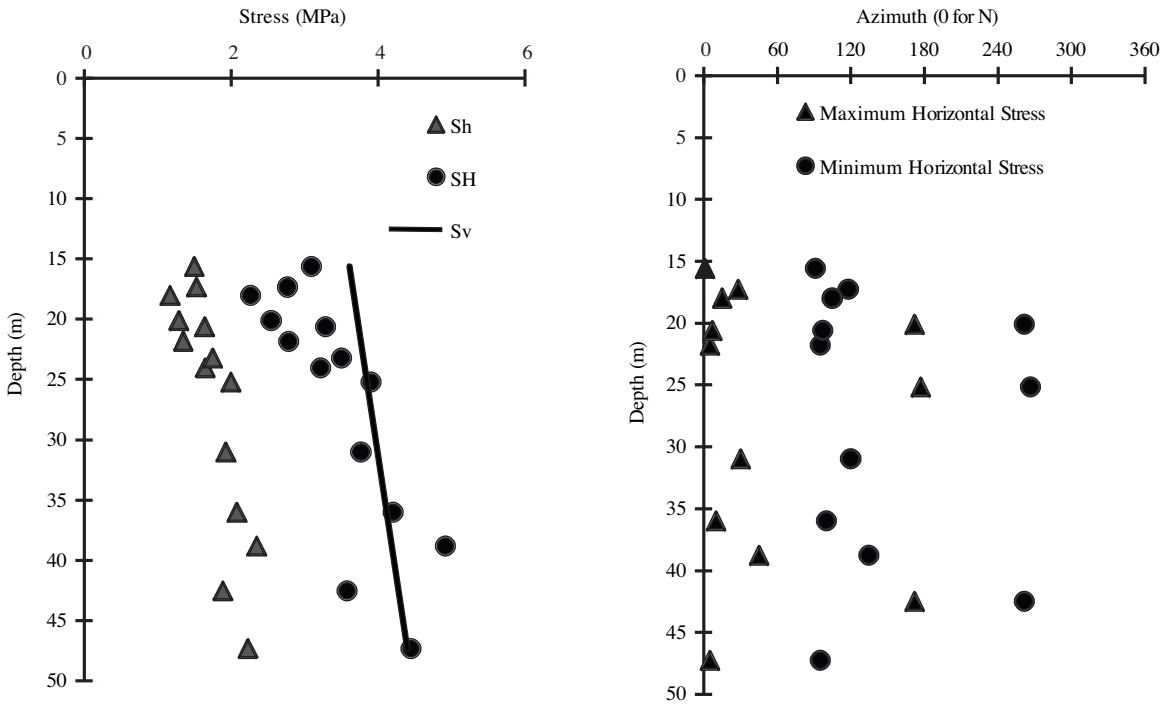


**Figure 13.** Principal stress interpretations at the YB station: (a) Principal stress vs. depth; (b) Principal stress orientation vs. depth.

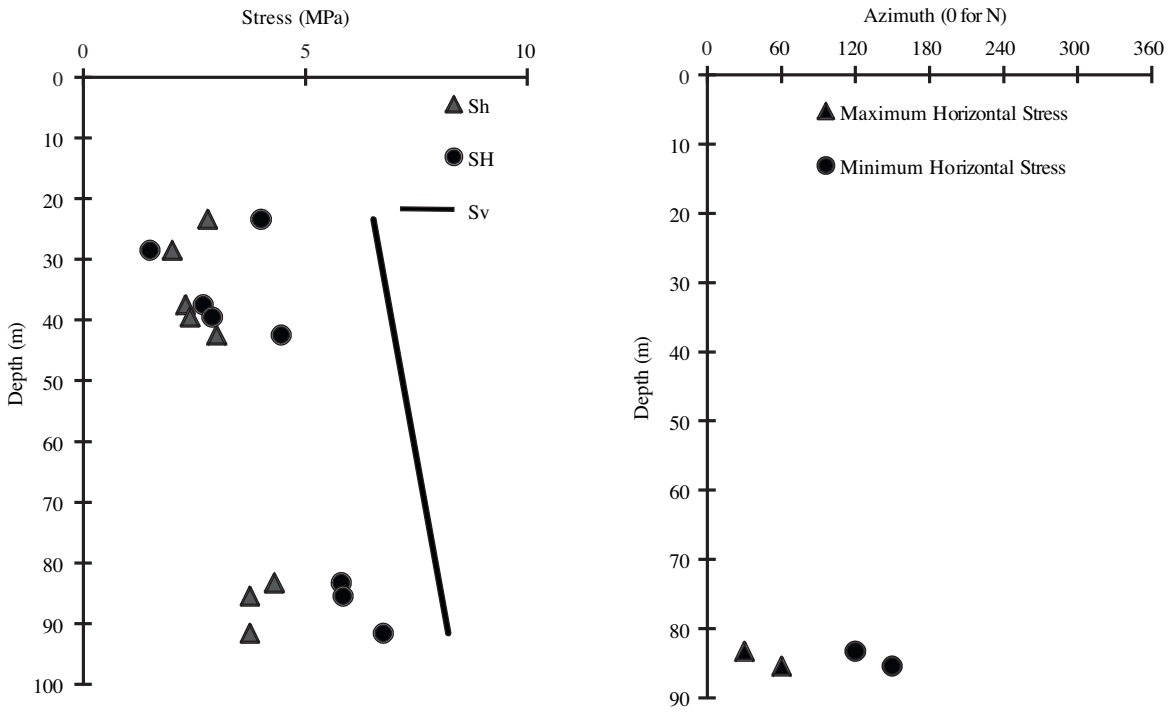


**Figure 14.** Principal stress interpretations at the T2 station: (a) Principal stress vs. depth; (b) Principal stress orientation vs. depth.

Because of the lower elevation of the LP station with respect to the river level and less overburden compared to the other stations, a horizontal stress is a maximum principal stress caused by tectonic effects. In contrast, at the YB and T2 stations, the vertical stress component is the maximum principal stress. In the other words, this study shows that at the lower penstock tunnels (LP station) the vertical stress, $\sigma_v$, due to the small weight of the overburden with given rock density is the intermediate principal stress, while in the tunnels located at the YB and T2 stations, $\sigma_v$ is the maximum principal stress.

### 5.4. Maximum horizontal principal stresses orientation

The hydraulic fracturing tests were conducted in both fractured and intact rocks. Regarding the fracture planes being induced, the impression packer is used for determining the actual principal stresses. As shown in Table 2., the measurements yield an orientation of the maximum horizontal stress, which is the same as most of the induced and pre-existing fractures, with strike direction of N 30° ± 5° (NE-SW). This direction is generally the same as directions indicated by focal mechanisms solutions from earthquakes (Figure 15). As shown in Figure 16, the strike direction of the maximum horizontal principal stress is obtained perpendicular to the general fault extension in the test location.

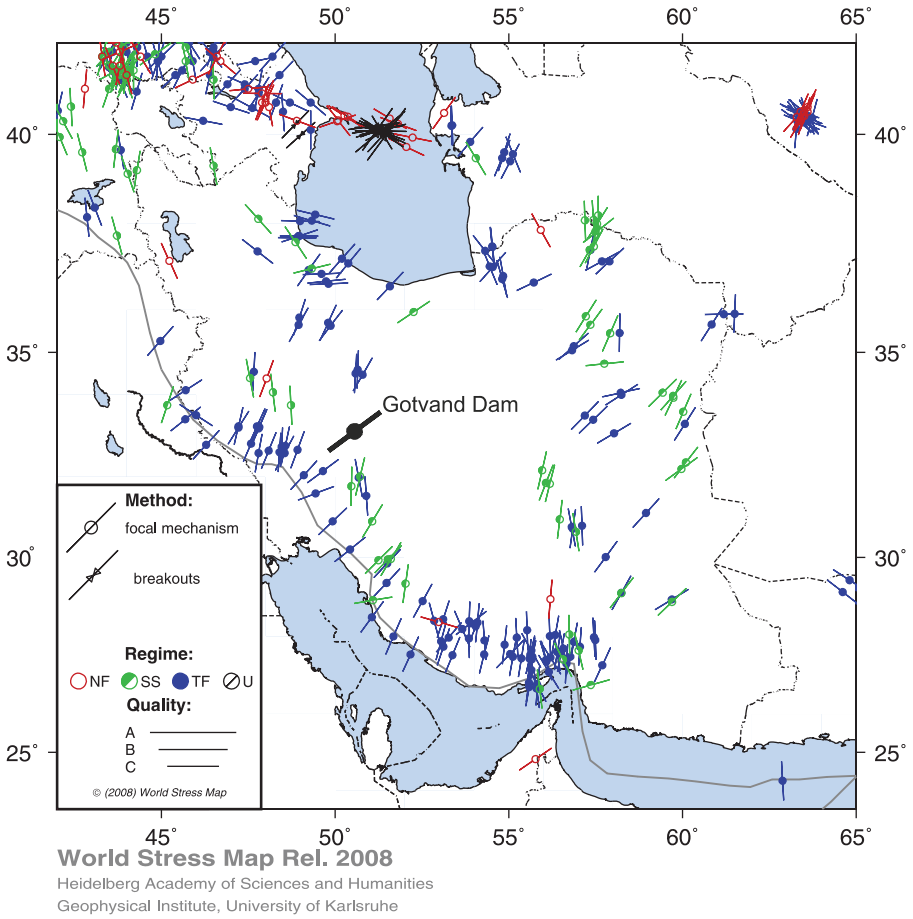


**Figure 15.** Directions indicated by HFT on Iranian focal mechanism solutions from earthquake map.

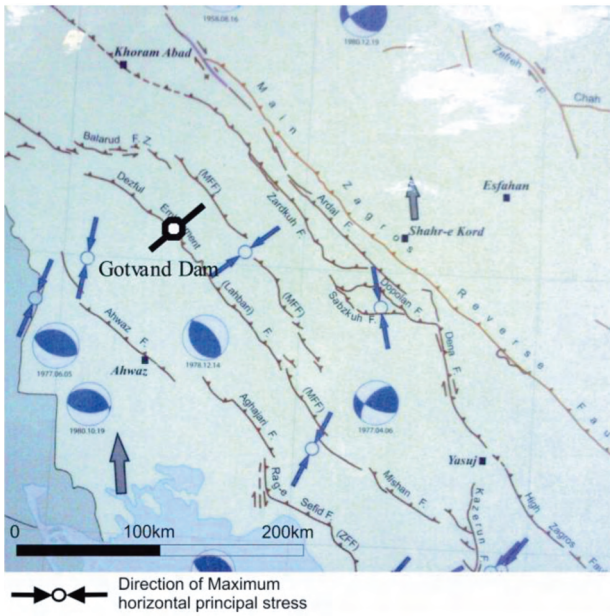


**Figure 16.** Directions indicated by HFT on Iranian fault system.

## 6. Conclusions

The HFT results at the Gotvand Dam site can be summarized as follows:

- Results of all hydraulic fracturing tests showed that all of the HFT and HTPF parameters ($P_c$, $P_r$, $P_{si}$, and $P_{co}$) increase with depth.
- To evaluate the maximum, intermediate, and minimum principal stresses, the Hubbert and Willis formula was used. The principal stress interpretations showed that due to the small weight of the overburden with given rock density at the LP station the vertical component of stress is the intermediate principal stress and a horizontal stress is a maximum principal stress caused by tectonic effects. In contrast, at the other stations, because of such high overburden, the vertical stress component is the maximum principal stress.
- The measurements yield an orientation of the maximum horizontal stress with strike direction of N 30° ± 5° (NE-SW). This direction is generally compatible with the directions indicated by focal mechanisms solutions from earthquakes. It is also found that the strike direction of most of the induced and pre-existing fractures are the same as the general fault extension in the test location.

## References

Ajalloeian, R., Fatehi, L. and Ganjalipour, K., "Evaluation of Hydrojacking and Hydrofracturing Behaviour in Aghajari Formation (Gotvand Dam Site Foundation), Iran", Journal of Geology and Mining Research, 3, 46-53, 2011.

ASTM D4645, "Standard Test Method for Determination of In situ Stress in Rock Using the Hydraulic Fracturing Method", 1992.

Baumgärtner, J. and Rummel, F., "Experience with "Fracture Pressurization Tests" as a Stress Measuring Technique in a Jointed Rock Mass", Int. J. of Rock Mech, Min. Sci. & Geomech. Abstr., 26, 661-671, 1989.

Cornet, F.H. and Julien, P.H., "Stress Determination from Hydraulic Test Data and Focal Mechanisms of Induced Seismicity", Int. J. Rock Mech. Min. Sci. & Geomech Abstr., 26, 235-248, 1989.

Gronseth, J.M. and Kry, P.R., "Instantaneous Shut-in Pressure and Its Relationship to the Minimum in Situ Stress", Proc. Workshop on Hydraulic Fracture Stress Measurements, Monterey, CA, 55-65, 1981.

Guo, F., Morgenstern, N.R. and Scott, J.D., "Interpretation of Hydraulic Fracturing Pressure: A Comparison of Eight Methods Used to Identify Shut-in Pressure", Int. J. Rock Mech. Min. Sci. & Geomech. Abstr., 30, 627-631, 1993.

Haimson, B.C. and Fairhurst, C., "In Situ Stress Determination at Great Depth by Means of Hydraulic Fracturing", Rock Mechanics—Theory and Practice, (ed.) W. H. Somerton, Am. Inst. Mining Engrg., 559-584, 1970.

Haimson, B.C. and Cornet, F.H., "ISRM Suggested Methods for Rock Stress Estimation—Part 3: Hydraulic Fracturing (HF) and/or Hydraulic Testing of Pre-Existing Fractures (HTPF)", Int. J. Rock Mech. & Min. Sci., 40, 1011-1020, 2003. Haimson, B.C., Lee, M.Y. and Song, I., "Shallow Hydraulic Fracturing Measurements in Korea Support Tectonic and Seismic Indicators of Regional Stress", Int. J. Rock Mech. & Min. Sci., 40 1243-1256, 2003.

Hanson, M.E., "The New Revised ASTM Standard and ISRM Suggested Method for Conducting Hydraulic Fracturing In Situ Stress Measurements", 57-OSE-A1150, 2004.

Hubbert, M.K. and Willis, D.G., "Mechanics of Hydraulic Fracturing", American Institute of Mining, Metallurgical, and Engineers Petroleum Transactions, 210, 153-166, 1957.

Jeffrey, R.G., Zhang, X. and Bunger, A.P., "Hydraulic Fracturing of Naturally Fractured Reservoirs", Thirty-Fifth Workshop on Geothermal Reservoir Engineering, Stanford University, Stanford, California, February 1-3, 2010. Available via:

http://pangea.stanford.edu/ERE/pdf/IGAstandard/SGW/2010/jeffrey.pdf

Kirsch, G., "Die Theorie der Elastizität und die Bedürfnisse der Festigkeitslehre", Zeitschrift des Vereines deutscher Ingenieure, 42, 797-807, 1898.

Klee, G. and Rummel, F., "Forsmark Site Investigation, Rock Stress Measurements with Hydraulic Fracturing and Hydraulic Testing of Pre-Existing Fractures", 2004. Available via:

http://www.skb.se/upload/publications/pdf/P-04-311webb.pdf

Shadizadeh, S.R., Habibnia, B.A. and Syllabee, R, "Investigation and Selection of Suitable Layers in Bangestan Reservoir for Hydraulic Fracturing Operation", Sharif University of Technology, Transactions C: Chemistry and Chemical Engineering, 16, 2, 149-160, 2009.

Ziaie Moayed, R., Pahlavan, B., Fazlavi, M. and Valinejad, N., "Hydraulic Fracturing Test in Gotvand Dam", 5th Engineering Geology and Environmental Science, Tehran, Iran, 2008.